ECOLOGY

Informing trait-based ecology by assessing remotely sensed functional diversity across a broad tropical temperature gradient

Sandra M. Durán[1]*, Roberta E. Martin[2], Sandra Díaz[3], Brian S. Maitner[1], Yadvinder Malhi[4], Norma Salinas[4,5], Alexander Shenkin[4], Miles R. Silman[6], Daniel J. Wieczynski[7], Gregory P. Asner[2], Lisa Patrick Bentley[8], Van M. Savage[7,9], Brian J. Enquist[1,9]

Spatially continuous data on functional diversity will improve our ability to predict global change impacts on ecosystem properties. We applied methods that combine imaging spectroscopy and foliar traits to estimate remotely sensed functional diversity in tropical forests across an Amazon-to-Andes elevation gradient (215 to 3537 m). We evaluated the scale dependency of community assembly processes and examined whether tropical forest productivity could be predicted by remotely sensed functional diversity. Functional richness of the community decreased with increasing elevation. Scale-dependent signals of trait convergence, consistent with environmental filtering, play an important role in explaining the range of trait variation within each site and along elevation. Single- and multitrait remotely sensed measures of functional diversity were important predictors of variation in rates of net and gross primary productivity. Our findings highlight the potential of remotely sensed functional diversity to inform trait-based ecology and trait diversity-ecosystem function linkages in hyperdiverse tropical forests.

INTRODUCTION

Understanding and anticipating the consequences of species loss for ecosystem properties and their benefits for humans define much biodiversity research (*1*, *2*). From small to large spatial scales, there is an urgent need for better monitoring and quantification of biodiversity. Measures of organismal traits are increasingly being used to characterize biological diversity and to predict how organisms will respond to disturbances, environmental conditions, and biotic interactions (*1*, *3*, *4*). It has been increasingly recognized that functional diversity, the range, value, and abundance of organismal traits, not the taxonomic richness, is an important predictor of the effect of biodiversity on ecosystem functioning (*5*–*7*). Extensive evidence from experimental and observational studies has shown that capturing the functional characteristics of a community is of particular relevance to predict ecosystem productivity and stability (*1*, *2*, *6*). Functional diversity has been proposed to mechanistically link species diversity with biogeochemical cycles (*1*, *3*), guide management and conservation (*1*, *2*), as well as to bridge the gap between field-based studies and satellite-based research (*4*, *8*).

Functional diversity is a multifaceted concept reflecting a variety of potential biotic and abiotic processes that operate at different scales—from local populations to wide geographical regions (*1*, *9*). Despite the increasing interest in functional trait approaches, much research on spatial variation of plant diversity continues to focus on changes in species richness (*10*, *11*). For example, many publications have evaluated the species-area relationship, and the increases in species richness with area are generally considered as a fundamental concept in biogeography (*11*). However, corresponding patterns in plant functional diversity are rarely assessed (*12*, *13*). Such measures may provide insights into the mechanisms that shape the composition and dynamics of ecological communities (*12*, *13*) and functioning of ecosystems (*1*, *3*, *4*).

Trait-based approaches have the potential to be more accurate than species-centered approaches because of the continuous nature of functional traits (*4*, *9*), but the usefulness and power of these approaches rely on the accurate characterization of traits and functional diversity. While a multitude of methods are available for quantifying functional diversity using field sampling (*9*, *14*–*16*), it is unclear whether they can be applied at different spatial scales. This uncertainty constrains the ability to generalize results or compare studies across scales (*9*). Remotely sensed measures of functional diversity have made it possible to quantify spatial variation in foliar traits across large environmental gradients (*17*–*22*). Imaging spectroscopy captures the reflectance of light from Earth's surface, generating continuous spectra from the visible to infrared wavelengths (*23*, *24*). These spectra can be directly linked to biochemical and morphological traits (*17*–*19*, *25*) and have been used to successfully predict foliar traits in different landscapes (*21*, *22*, *25*, *26*).

There are two challenges in linking traits to ecosystem functioning using remote sensing: The first challenge is how to quantify the continuous distribution of traits across scales to map and model functional diversity across biogeographical gradients. Field-based trait studies generally characterize functional diversity by representing each species by average trait values (*9*, *27*). Often, trait values come from global datasets with trait values measured elsewhere. This approach, implicitly, assumes that interspecific trait variability is larger than intraspecific trait variability, but theoretical and empirical research has shown that intraspecific trait variability, measured locally, is an important component of community assembly and how species respond to changing climate and species composition (*27*, *28*). Thus, it remains a challenge to quantify functional diversity in a way that includes both intra- and interspecific trait variation across different spatial scales (*9*, *27*, *28*).

[1]Department of Ecology and Evolutionary Biology, University of Arizona, Tucson, AZ 85721, USA. [2]School of Geographical Sciences and Urban Planning, Center for Global Discovery and Conservation Science, Arizona State University, Tempe, AZ 85287, USA. [3]Instituto Multidisciplinario de Biología Vegetal (IMBIV), CONICET and FCEFyN, Universidad Nacional de Córdoba, Casilla de Correo 495, 5000 Córdoba, Argentina. [4]Environmental Change Institute, School of Geography and the Environment, University of Oxford, Oxford 0X1 3QY, UK. [5]Sección Química, Pontificia Universidad Católica del Perú, Avenida Universitaria 1801, San Miguel, Lima 32, Perú. [6]Department of Biology, Wake Forest University, Winston-Salem, NC 27109, USA. [7]Department of Ecology and Evolutionary Biology, University of California, Los Angeles, 612 Charles E Young Drive South, Los Angeles, CA 90095, USA. [8]Department of Biology, Sonoma State University, 1801 East Cotati Avenue, Rohnert Park, CA 94928, USA. [9]Santa Fe Institute, 1399 Hyde Park Road, Santa Fe, NM 8750, USA.
*Corresponding author. Email: smduranm@gmail.com

Imaging spectroscopy provides a spatially continuous quantification of plant traits incorporating the within- and among-community variation of traits at different spatial and temporal scales (*17*–*19*, *25*, *26*).

The second challenge is to assess whether variation in functional diversity across large environmental gradients can predict forest productivity using biodiversity–ecosystem functioning relationships (*1*, *6*, *7*). Measures of remotely sensed functional diversity are limited and continue to be incomplete and nonrepresentative taxonomically or geographically (*20*, *21*). For example, our knowledge of the distribution of functional traits across plant species is sparse, with relatively large data gaps in tropical regions [(*19*, *20*), but see (*8*, *22*, *29*, *30*)]. Tropical forests are very important in the global carbon budget, representing 20% of global terrestrial carbon stocks and 30% of global terrestrial primary productivity (*31*), but it remains unclear what controls variation in forests productivity in tropical regions. Although several studies have quantified forest productivity in lowland tropical regions, the carbon cycle of tropical montane forests is only starting to be explored (*32*–*34*), and it is still not well understood what is the relative importance of climate and functional characteristics on rates of carbon capture and gain in tropical montane forests (*33*, *34*).

Here, we present a general framework to scale up remotely sensed metrics of functional diversity to assess prominent hypotheses in trait-based ecology and the role of functional diversity in influencing ecosystem processes (Fig. 1). First, building on previous work (*22*), we evaluated the role of airborne imaging to quantify spatial scaling in functional diversity (Fig. 1A) across a broad temperature gradient. Next, to assess the role of differing hypotheses that structure variation in trait diversity, we assessed the shape of the distribution of functional diversity across spatial scales (Fig. 1, B and C). Last, we test the ability of remotely sensed trait diversity to test the hypothesized linkages between functional diversity and ecosystem productivity [e.g., (*5*, *7*)] (Fig. 1D). We focused our study on trait and ecosystem measures from nine 9-ha tropical forest sites that span a 3300-m elevation range and approximately 17°C gradient in mean annual temperature (MAT) in the Peruvian Andes (see table S1 and fig. S1) (*22*, *33*). We integrated field and airborne data of canopy traits and ecosystem productivity (*8*, *22*, *32*) to assess the relationship between functional diversity and forest productivity along the elevation gradient.

We defined functional diversity in a broad sense including single- and multitrait diversity indices. Single traits correspond to the community mean trait (CMT) values of leaf physiological traits that were well mapped along this gradient from the airborne spectroscopy data (*22*). The selected traits were leaf dry mass per unit area [LMA; balancing leaf construction cost versus growth potential (*35*)], which is a key trait related to photosynthesis and tree growth (*33*); leaf chlorophyll (Chl) facilitating light capture and photo-protection (*36*); leaf water content (Water) underpinning photosynthesis and primary production (*36*); and nonstructural carbohydrates (NSC), which support long-lived tissues and are important for tree survival (*37*). The CMT values were calculated for each site along the elevation gradient using 4-m^2 pixel size and are not weighted by abundance. Multitrait indices were estimated using two indices: functional richness (FRic), which represents the amount of niche space occupied by the community, calculated as the convex hull volume of the four canopy traits, and functional divergence (FDiv), which quantifies how sample points diverge in their distances from the center of gravity in the multitrait functional space (*14*, *15*). High values of FRic indicate a wide range of trait values in the functional space. High values of FDiv indicate high niche differentiation and suggest low competition (*9*). For ecosystem measures, we used ground-based data on gross and net primary productivity (NPP) previously measured along this gradient, constituting one of the most comprehensive datasets of carbon productivity, allocation, and storage in tropical forests (*32*).

We hypothesized that (i) FRic and FDiv decrease with elevation because environmental constraints at higher altitudes reduce the range of trait variation and reduce the differentiation among traits (Fig. 1A) (*35*). Previous research (*22*) has shown that at lower elevation, single-trait values will be more associated with higher resource acquisition rates, while at higher elevations, as the abiotic environment becomes more stressful, traits will be more associated with conservative resource characteristics (*22*, *36*). In addition, we assessed the hypothesis that (ii) community assembly processes will be influenced by spatial scale (Fig. 1B) (*13*, *38*). Specifically, increasing environmental filtering (trait convergence) will be more pronounced at larger spatial scales (*38*, *39*) but also more prevalent in colder environments in increasing elevations (Fig. 1C (*35*). Further, biotic interactions will be more pronounced locally, resulting in increased trait divergence at smaller spatial scales but more prevalent at lower elevations (Fig. 1C) (*39*). Last, we expect that (iii) single- and multitrait metrics of functional diversity will be strong predictors of variation in rates of ecosystem productivity along elevation (Fig. 1D) (*7*).

RESULTS

Changes of functional diversity along elevation

Consistent with the hypothesis of increased functional convergence in colder climates (*35*), FRic declined with elevation and temperature, while FDiv did not change (Fig. 2). Similar to FRic and as measured previously (*22*), single-trait CMT plot values of LMA, NSC, and Chl calculated from the 4-m^2 pixel size were linearly related to elevation (see fig. S2). The lowest elevation sites showed a wider range of within-community variation in FRic (Fig. 2A) and high spatial variation within plots (see fig. S3). In contrast, FDiv showed a narrower range of within-community variation (Fig. 2B), with little spatial variation within sites along the elevation gradient (see fig. S3).

Effect of spatial scale on multitrait diversity indices

FRic changed as a function of spatial scale, with increases in FRic with sampled area (Fig. 3A). The measured values of FRic in most sites were scale dependent and were significantly lower than expected by chance. These results show strong convergence in FRic at the site scale (e.g., FRic among close neighbor pixels are more similar; Fig. 3A) using single- and multitrait measures of FRic (fig. S4). FDiv did not change with spatial scale and showed idiosyncratic patterns across sites (Fig. 3B) for both single- and multitrait measures of FDiv (fig. S5). In most sites, FDiv-area curves did not differ from the expected value as FDiv-area curves overlap with expectation from the null model (e.g., FDiv is randomly distributed within sites; Fig. 3B). Fitting a logarithmic model to the FRic-area relationships [FRiv versus natural log (area); see Materials and Methods], we found that slopes range from 0.10 to 0.32. After controlling for the scale dependency, the rate of change of FRic and FDiv (e.g., the slope) did not change with elevation (Fig. 4, A and B). We assessed community assembly processes across the elevation gradient by calculating the standardized effect sizes (SES) between null and observed communities, with SES < 0 indicating the prevalence of environmental filtering (trait convergence), while SES > 0 suggesting stronger biotic interactions (trait divergence) (see Fig. 1C and Materials and Methods). We found that environmental filtering was an important

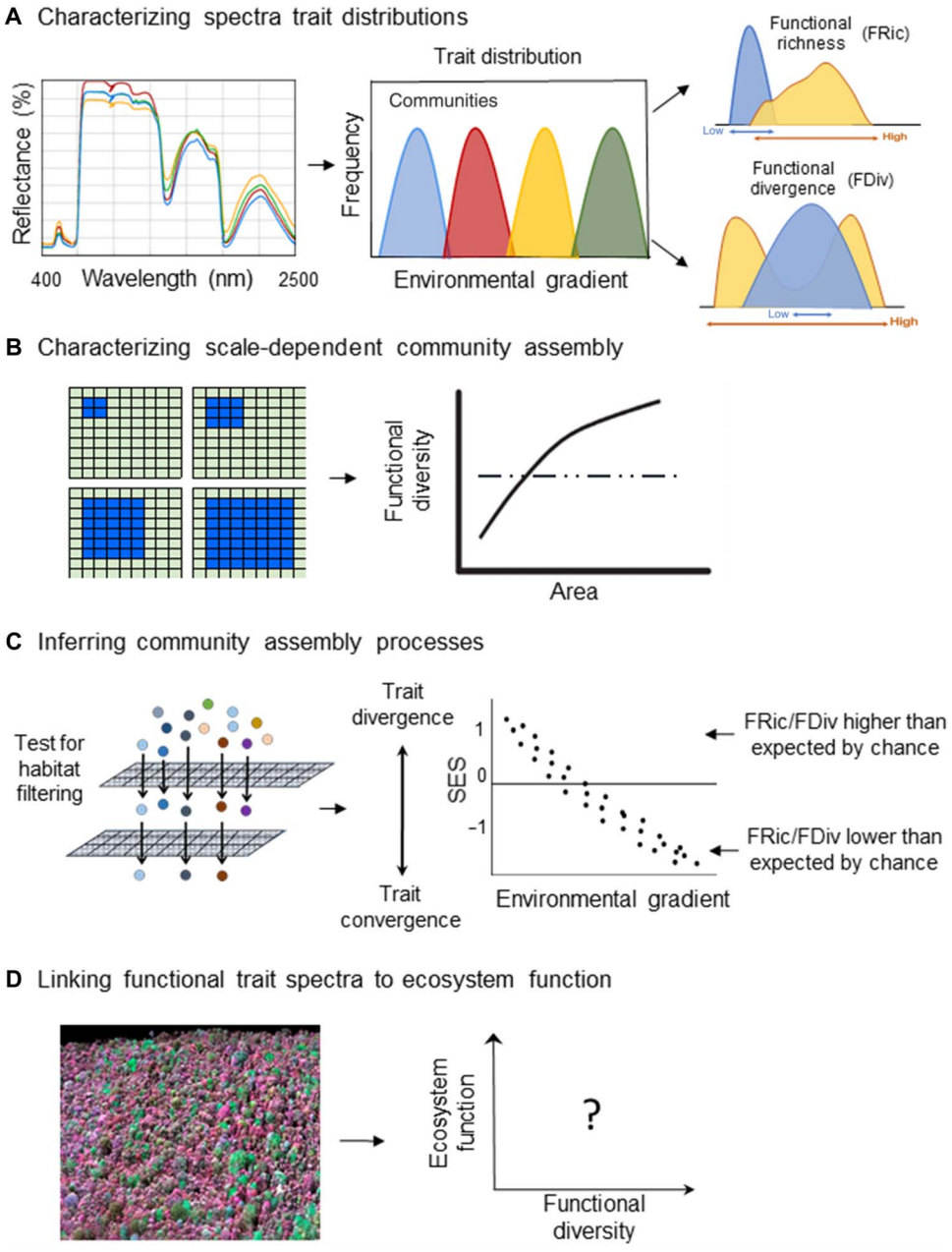

Fig. 1. Approach to use remotely sensed functional diversity to inform trait-based ecology. (**A**) Trait distributions are derived from imaging spectroscopy spanning the visible, near-, and short-wave-infrared wavelengths (400 to 2500 nm). Functional diversity indices are quantified from trait distributions to understand how plant communities change across environmental gradients. We estimated functional richness (FRic) and functional divergence (FDiv). FRic corresponds to the convex hull volume and represents the trait space occupied by a community. When this volume is narrow, FRic is low (blue community), and when FRic is large, the range is wider (yellow community). FDiv represents how sample points diverge in their distances from the center of the multitrait functional space. Large values of FDiv indicate high trait differentiation within a community (yellow), and low values indicate lower divergence (blue). (**B**) The scale dependency of community assembly processes is evaluated by assessing variation in functional diversity across spatial scales. Functional diversity either changes with area (bold line) or is scale invariant (dashed line). (**C**) Community assembly processes are disentangled by testing for the relative importance of trait convergence (environmental filtering) and trait divergence (biotic interactions). (**D**) Functional diversity effects on ecosystem processes are tested by examining whether remotely sensed diversity indices are related to forest productivity.

driver of the range of trait variation (FRic) within each community and across sites (Fig. 4C). In contrast, patterns of FDiv across elevation suggest that some sites might be influenced by environmental filtering, while others may be more strongly affected by biotic interactions (Fig. 4D).

Linkages of trait diversity and GPP and NPP

Remotely sensed multitrait functional diversity and single-trait CMT components were related to forest productivity along the elevation gradient. Multitrait FRic and CMT values of LMA, Chl, and NSC were all significant predictors of NPP and gross primary productivity (GPP)

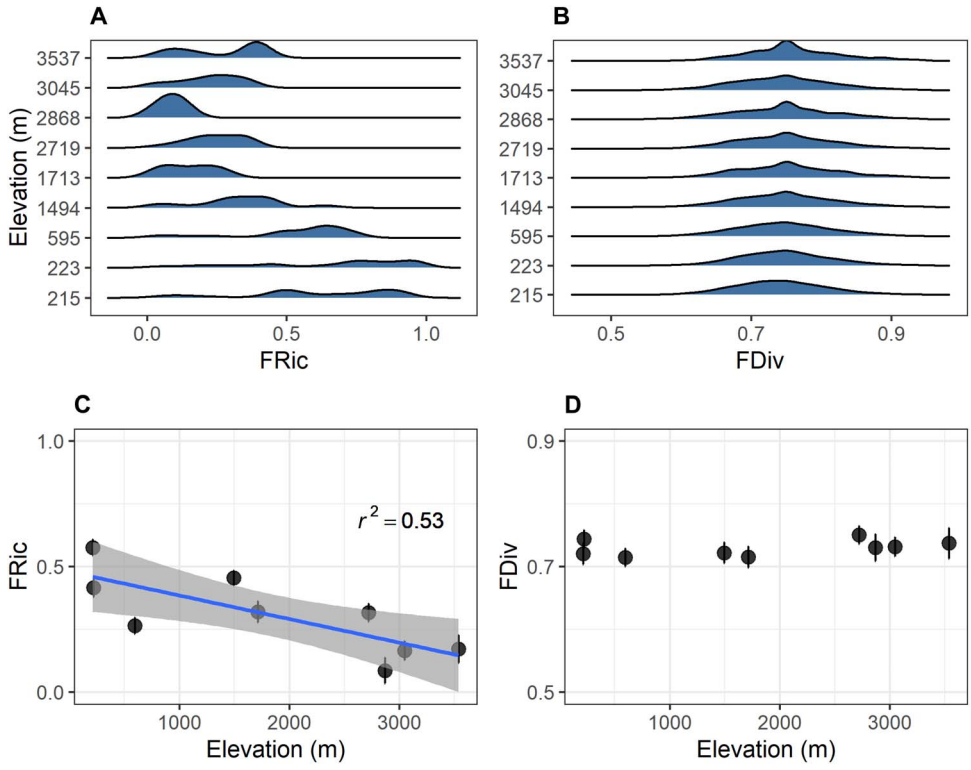

Fig. 2. Variation of remotely sensed functional diversity indices across sites along elevation. Distribution of trait diversity indices within and among sites along elevation are shown for (**A**) FRic and (**B**) FDiv. Relationships between mean values per site of FRic and FDiv and elevation are indicated in (**C**) and (**D**), respectively. Black circles represent average values of FRic and FDiv in each site, and the dark vertical lines are their 95% confidence intervals. Significant regression fit is shown by a solid blue line, with gray strips showing the 95% confidence intervals of the fit and r^2 indicating the amount of variation explained by elevation.

across sites (Fig. 5). Model selection results indicated that MAT and FRic were important predictors of GPP along the elevation gradient, explaining over 40% of the variation in GPP. NPP, on the other hand, was more strongly related to MAT, elevation with CMT LMA being the only single-trait index selected in the final models (Table 1). In contrast to FRic, FDiv and foliar water content were not correlated with ecosystem production (Fig. 5 and Table 1).

DISCUSSION

The Amazon-Andes elevation gradient studied here provides a natural laboratory to investigate covariation in plant functional diversity and ecosystem processes under highly contrasting environmental conditions (*33*). Our approach focused on remotely sensed traits to understand how functional diversity of tree communities change with elevation and spatial scale, and the linkages between this diversity and ecosystem productivity.

Trait diversity across environmental gradients

FRic, a multitrait measure of the range of trait variation within a community, declined with increased elevation. This shift appears to correspond mostly to reductions in mean temperature with elevation from 24° to 9°C, since radiation and precipitation do not show overall trends with increasing elevation in our study area (*22*, *33*). Higher values of FRic may be related to high resource availability, more stable climate, higher solar radiation, and, in general, more favorable conditions for tree communities with different leaf syndromes to establish at lower elevations (*22*, *29*, *35*). This is also evident by looking at FRic distributions; at higher elevations, the range of variation tends to be narrower than the range of values in the lowland sites (Fig. 2A). FDiv, which represents how spread out or how clumped the traits are represented in niche space (*14*), did not change along the elevation gradient. Any directional variation in FDiv may have been masked due to the high within-site variation found on the trait distributions (Fig. 2B and fig. S5). This is consistent with changes in CMT values of the four leaf traits. We found traits associated with higher acquisition rates at lower elevations, represented by low values of LMA and NSC (fig. S2) and high values of Chl. In contrast, at higher elevations, we found high NSC and LMA, which tend to be associated with plant resource conservation strategies under unfavorable growing conditions. This transition from acquisitive to conservative strategies agrees with predictions for how the leaf economics spectrum constrains plant strategies in cold and less productive environments (*35*, *39*) and with previous findings using remotely sensed traits across the Peruvian Amazon (*29*) and along this gradient (*22*, *30*).

Airborne imaging and foliar spectroscopy are becoming increasingly available at different scales, but little research has been conducted to estimate functional trait diversity from spectral data (*20*, *21*). Combining airborne imaging and field-based data, it is possible to derive remotely sensed traits and map and quantify functional diversity indices (Fig. 1). Nonetheless, the retrieval of plant traits using this approach, specifically in tropical forests, presents some limitations. Tropical forests show an exceptionally high structural and taxonomic diversity and canopy inaccessibility, which made it difficult to sample all tree species within the field sites (*40*). Imaging spectroscopy can overcome limitations in field-based sampling by providing a greater spatial coverage of canopy properties at the stand level. However, matching field-based

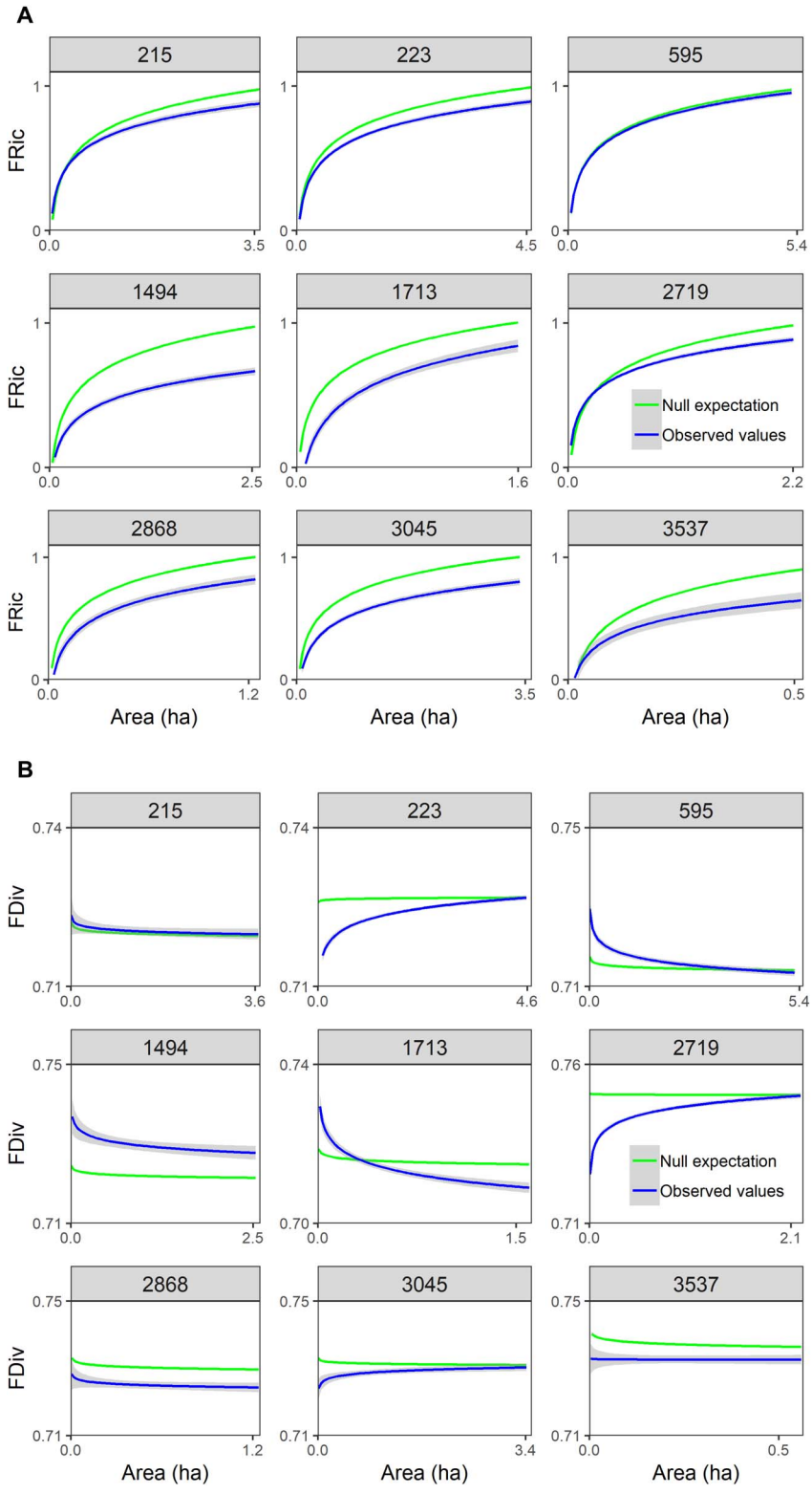

Fig. 3. Functional diversity–area relationships across sites. Scale dependency of two functional diversity measures across elevation in the nine study sites arrayed along the elevation gradient. (**A**) FRic and (**B**) FDiv. Curves represent the fit of functional diversity versus the natural log (area), green lines represent the fit for remotely sensed values, and blue lines represents the fit for simulated communities (e.g., null models; see the main text). Observed values of FRic and FDiv lower than fitted lines of the null models indicate strong environmental filtering at the site scale (e.g., trait convergence). Observed values of FRic and FDiv that are above the null expectations suggest that plant communities may be constrained by biotic interactions (e.g., trait divergence). Overlapping curves indicate no difference between simulated and measured indices and that traits are randomly distributed at the site scale.

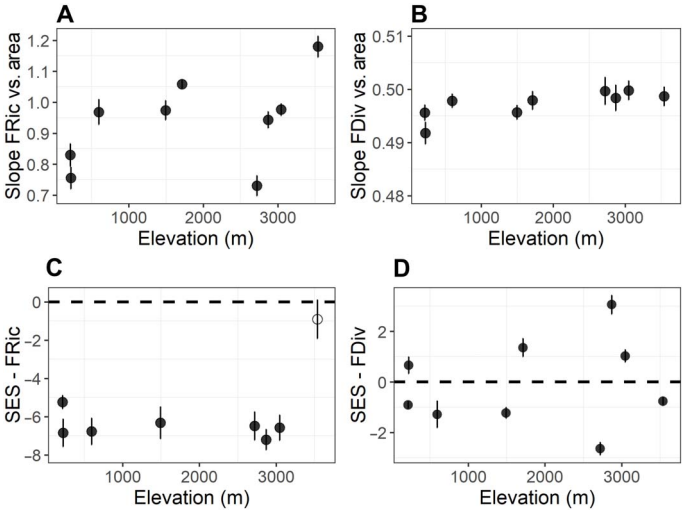

Fig. 4. Changes in FRic and FDiv along elevation after controlling for scale dependency. (**A** and **B**) Relationship between the slope of FRic-area and FDiv-area and elevation. These slopes were calculated by fitting a log-log relation of each index with area in each site. Bars indicate 95% confidence intervals. (**C** and **D**) Standardize effect sizes (SES) of FRic and FDiv along elevation. The dashed line represents the zero value. SES that is significantly greater than, smaller than, or approaching zero indicate significant trait divergence, trait convergence, or random distribution, respectively. Mean SES values and 95% confidence intervals are shown for each site. Black circles indicate significant differences ($P < 0.05$) between simulated and observed communities, while open circles indicate nonsignificant differences based on Wilcoxon signed-rank tests.

and airborne imaging data remains challenging, as there is an inherent mismatch in scale that cannot be directly overcome due to the inability to sample the whole plot area using field sampling (*22*, *40*). This mismatching can also affect the predictability of remotely sensed traits from field data limiting our analysis.

Our study focused on four plant traits that can be accurately measured from airborne imaging (*20*, *22*), but other traits not included in this analysis may have an influence in community assembly processes or influence the rates of forest productivity. Future research should develop methods to map the distribution of plant traits through the integration of global datasets (*41*–*43*), field-based methods (*16*), and the spectranomics approach (*19*) using hyperspectral sensors. A recent study showed that an integrated framework incorporating plant trait databases, remotely sensed data, and climatic parameters is useful to develop trait maps at a global scale (*26*). The spectral resolution of plant traits in this framework, however, is still limited for the lack of high-fidelity hyperspectral data at a global level. The spaceborne missions such as ENMap [Environmental Mapping and Analysis Program (*44*)] and HyspIRI (Hyperspectral Infrared Imager) are promising to provide high spatial and spectral resolution to derive plant traits. This will likely provide a more direct path to estimate plant functional diversity and will allow the development of methods to scale up in situ trait measurements to regional and continental scales (*26*, *45*).

Scale-dependent community assembly

The functional diversity–area relationship along the elevation gradient provided evidence for scale-dependent trait diversity (*21*). Specifically, FRic increased with area. This positive FRic-area relationship agrees with patterns of species-area curves in other tropical forests (*10*) and other studies assessing FRic-area associations using field-based data (*10*, *12*) and remote sensing (*21*). There was large variation in the slope of this relationship across sites, which highlights the contribution of local factors in explaining trait variation (Fig. 4A). Comparisons of simulated and observed communities indicated that FRic values were lower than expected, suggesting a strong signal of trait convergence dominates in the whole study area. Temperature, which is highly correlated with elevation along this gradient (*22*), is strongly associated with trait variation across these communities and constrains the range of trait space at higher elevations (*35*, *39*). Other abiotic factors that may constrain the range of traits within and across communities are precipitation and nutrient availability. At middle elevations, high soil water content due to high rainfall (over 5000 mm in sites between 1500 and 2000 m of elevation; table S1) may affect the spatial variation of nutrient availability constraining the range of traits in the community.

We did not find scale dependency on FDiv along elevation. FDiv can change independently of FRic and represents the degree of trait divergence in a community (*15*). Other studies have also found that FDiv follows idiosyncratic patterns with area (*21*). As area increases, the range of traits can increase as we found with FRic, but the relative abundance of unique traits does not increase proportionally. When some traits become dominant, they become more representative in the trait space and reduce the within-community variation of traits, thus decreasing the FDiv (*14*, *15*). Our patterns of FDiv show that although temperature has an influence on some functional traits (e.g., LMA), trait divergence among tree species is driven by other factors such as precipitation or radiation that does not change in parallel with elevation as does temperature. Along elevation, SES values of FDiv were positive and negative, indicating that biotic interactions may be stronger in some sites, while environmental filtering may be more important in others. High FDiv values suggest a high degree of niche differentiation (*14*). Biotic interactions may be related with microsite conditions related with competition for water or light among species (*46*). Abiotic filtering is related to changes in temperature, soil moisture, and local disturbances, since some sites in the gradient are exposed to regular flooding or landslides, which may influence the differentiation of traits across individuals (*22*, *46*).

Multiple interacting factors can influence species diversity and the distribution of traits within communities. The relative importance of the factors that result in species sorting (e.g., competition and facilitation) is scale dependent (*12*, *13*, *38*, *39*). Our approach built on functional diversity indices derived from imaging spectroscopy integrates both the within- and between-community trait variation and the frequency of trait values. These findings are consistent with the expectation, long-assumed (*38*) but rarely assessed within and across communities, that functional diversity is constrained by strong trait-environment matching. Nonetheless, these conclusions have been based on observations of trait ranges that do not often incorporate within-community variation. We found, when measurements incorporate the within and among trait variation across species-rich sites, the observed functional diversity appears to be highly constrained (see Fig. 4A). As a result, our approach can begin to assess scale dependency of trait diversity, including the FRic and FDiv of a single trait (see figs. S4 and S5). In doing so, we can start to disentangle the relative importance of ecological processes shaping community assembly within and across sites. Spatial variation of trait diversity facilitates the assessment of the ecological processes shaping community assembly across large environmental gradients. Further, using remotely sensed traits can complement field-based approaches, as it incorporates within- and across-community variation in trait diversity, which is essential to elucidate mechanisms of community assembly related to biotic interactions (*13*, *21*, *38*, *39*).

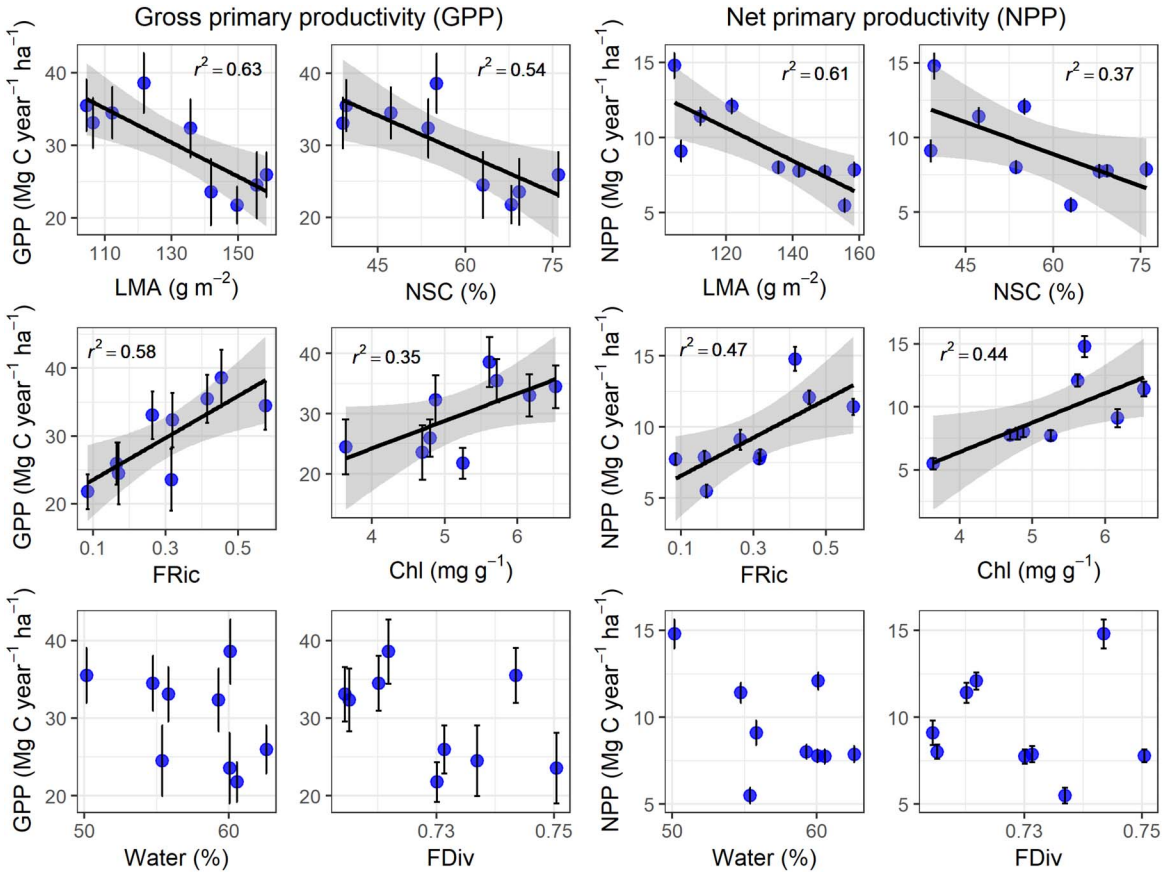

Fig. 5. Variation on rates of NPP and GPP across sites with remotely sensed diversity indices. Single-trait indices correspond to the CMT values of percent of water, NSC, leaf mass per unit area (LMA), and percent of chlorophyll (Chl). Multitrait indices, FRic, and FDiv are calculated using these four traits. Black lines represent linear regression fits, blue circles represent each study site, black lines indicate the standard error of GPP or NPP in each site, and the gray strips are the 95% confidence intervals of the regression fit. Percent of explained variation (r^2) by each diversity index is shown for all significant relationships ($P < 0.05$). GPP, gross primary productivity; NPP, net primary productivity.

Functional diversity effects on ecosystem productivity

We found that single- and multitrait diversity indices were important predictors of ecosystem productivity. CMT values of LMA and NSC along with FRic were significantly related to GPP and NPP (Fig. 5). Model selection results, however, indicated that CMT LMA, elevation, and MAT were among the best predictors of NPP rates, while FRic, CMT LMA, and MAT were selected in the best models explaining rates of GPP (Table 1). LMA is one of the most important traits related with plant resource acquisition, specifically the integration of light interception and plant growth (*35*, *46*). Allocation of NSC is associated with tree growth and reserves to survive in cold temperatures at high altitudes (*37*). The fact that FRic was selected as a strong predictor of GPP, but not NPP, suggests that the variation in GPP may be influenced by more than one trait, not mainly LMA, as was the case for NPP. Although we are unable to disentangle the relative importance of temperature and traits on rates of GPP and NPP due to our small sample size, overall, our analyses suggest that functional trait differences in tree communities may explain rates of ecosystem productivity along the elevation gradient. This is consistent with other studies in the same elevation gradient, which have found that rates of GPP and NPP were better explained by incorporating traits such as plant size or plant biomass using field-based methods (*33*). A semimechanistic model that evaluated the relative importance of climate, stand structure, and traits along the same elevation gradient found that models that incorporated field-based measured traits and solar radiation explained more variation in the rates of NPP and GPP than climate alone (*34*).

There is an increasing need to improve our ability to predict how climate change affects biological diversity and ecosystem properties. Increasing evidence has shown that both ecosystem productivity and plant functional traits show spatial variation across the landscape in tropical and temperate forests (*47*, *48*), but it remains unclear whether variation in productivity is explained by the variability of traits or by variation in environmental drivers (e.g., temperature and radiation) (*32*). Moreover, it remains unclear how we can scale up the trait-productivity relationships from local to landscape or continental scales (*47*). Our results show the potential of remotely sensed traits to explain variation of forest productivity at regional scales. Furthermore, as trait diversity is scale dependent, its effects on ecosystem productivity may also change with spatial scale. Future research should focus on understanding the scale dependency on the relationships between functional diversity and ecosystem productivity in tropical forests. This could be done by combining in situ observations of plant traits from global databases (*41*–*43*) and satellite data on ecosystem productivity from satellite data such as MODIS (Moderate Resolution Imaging Spectroradiometer), which provides global spatial coverage (*48*). This should, in turn, improve the new generation of dynamic global vegetation models using traits as input to understand climate change impacts (*34*, *49*).

Table 1. Results of the effect of remotely sensed functional traits and climate on NPP and GPP. For each model, standardized regression coefficients (β), SE, the second-order Akaike's Information Criterion (AICc), and the differential AICc (ΔAICc) are shown. r^2 is shown for significant relationships ($P < 0.05$). Best models (ΔAICc ≤ 2) are in bold. Single-trait indices correspond to the CMT values of percent of water, NSC, LMA, and percent of Chl. Multitrait indices, FRic, and FDiv were calculated using these four traits.

	NPP (Mg C year^{-1} ha^{-1})					GPP (Mg C year^{-1} ha^{-1})				
	β	SE	r^2	AICc	ΔAIC	β	SE	r^2	AICc	ΔAIC
Elevation (m)	−2.1	0.6	0.66	44.5	**0.1**	−3.8	1.4	0.51	61.4	3.3
MAT (°C)	6.5	1.7	0.66	44.4	**0**	13.8	3.7	0.66	58.0	**0**
Mean annual rainfall (mm)	0.8	2.3		54.0	9.6	7.3	4.0		64.3	6.3
Solar radiation (GJ m^{-2} year^{-1})	9.5	7.1		52.1	7.7	25.8	13.9	0.33	64.1	6.1
LMA (g m^{-2})	−14.1	3.8	0.66	44.6	**0.2**	−30.1	8.2	0.66	58.1	**0.1**
NSC (%)	−7.8	3.3	0.44	48.9	4.5	−18.9	6.2	0.58	60.2	**2.2**
Chl (mg g^{-1})	11.8	4.3	0.52	47.6	3.2	22.3	10.1	0.41	63.0	5.0
Water (%)	−23.4	12.9		50.7	6.3	−38.2	30		65.9	7.8
FRic	3.2	1.3	0.45	48.7	4.3	8.2	2.5	0.66	58.1	**0.1**
FDiv	−3.8	62.7		54.2	9.8	−173	116		65.3	7.3

MATERIALS AND METHODS

Study area

Our study was conducted using nine sites along an Amazon-Andes elevation gradient from 215 to 3557 m above sea level (fig. S1). Two sites were located in the Tambopata River basin of the Peruvian Amazon (TAM-05 and TAM-06). Another site was at the transition from lowland to submontane (PAN-02), and the remaining six sites were in montane landscapes in the region of Cusco (1527 to 3537 m above sea level) (*20*, *24*). The sites range in temperature from 25.2°C at the lowest elevation site to 9.0°C at the highest elevation site and show variation in solar radiation, soil moisture, and precipitation (table S1).

Field-based functional traits

Traits of plant species were measured from April to November 2013 as part of the CHAMBASA (Challenging Attempt to Measure Biotic Attributes along the Slopes of the Andes) project. A detailed description of field sampling techniques is provided elsewhere (*22*), but here, we provide an overview. One hundred eighty tree species were sampled, which accounted for 80% of total basal area per site. For each species, five individual trees in upland sites and three individual trees in lowland sites were sampled. Collection of leaf samples was conducted using tree climbing techniques to cut branches at the top of the canopy. Two branches of ≥1 cm diameter were sampled for each tree, with a total of 1025 branches sampled from 620 trees. Fully expanded leaves were randomly selected for determination of leaf LMA and leaf water concentration (Water), NSC, and leaf content of Chl following standard protocols (*19*, *36*). We selected these four traits because they can be remotely sensed and have shown variation across the elevation gradient (*22*).

Remotely sensed plant traits

Maps of plant traits LMA, Water, NSC, and Chl were generated and published by airborne imaging that was acquired in August 2013 to coincide with the campaign using the Carnegie Airborne Observatory-2, which included a high-fidelity visible-to-shortwave infrared (VSWIR) imaging spectrometer and a dual-laser waveform light detection and ranging (LiDAR) using the technique detailed by Asner *et al.* (*50*). Data were collected over each site from an altitude of 2000 m above sea level, an average flight speed of 55 to 60 ms^{-1}, and mapping swath of 1200 m (*40*, *50*). The VSWIR spectrometer measures spectral radiance in 427 channels spanning the 350- to 2510-nm wavelength range in 5-nm increments (full width at half-maximum). The spectrometer has a 34° field of view and an instantaneous field of view of 1 mrad. From 2000 m above sea level, the spectral data were collected at 2.0-m ground sampling distance, or pixel size, throughout the region. The LiDAR has a beam divergence set to 0.5 mrad and was operated at 200 kHz with 17° scan half-angle from nadir, providing swath coverage similar to the spectrometer. The LiDAR point density for this mapping study was 4 laser shots m^{-2}. The LiDAR data were used to precisely ortho-geolocate the VSWIR data and determine three-dimensional locations by using a digital terrain model and a 10 m × 10 m kernel passed over each flight block, with the lowest elevation estimate in each kernel assumed to be ground. Subsequent points were evaluated by fitting a horizontal plane, and the process was repeated until all points within the block were evaluated (*40*). These inputs were used to atmospherically correct the radiance imagery using the ACORN-5 model. Reflectance imagery was also corrected for brightness gradients using a bidirectional reflectance distribution function.

The VSWIR data were corrected from raw digital number values to radiance (W sr^{-1} m^{-2}) using radiometric calibration coefficients and spectral calibration. This method consists of processing the VSWIR and LiDAR data to develop a suitability map based on filtering data with vegetation height ≥2.0 m, minimizing intra- or intercanopy shade in the VSWIR pixel based on sun-sensor geometry from the LiDAR positioning data, and normalized difference vegetation index ≥0.8 (*22*). Together, these filters provided a pixel-by-pixel suitability map from which spectral reflectance can be selected for further analysis. Following filtering, the spectra were convolved to 10-nm bandwidth

and a brightness-normalization adjustment. This reduced the contribution of varying leaf area index to chemometric determinations of foliar traits from remotely sensed data. The resulting spectra were trimmed at the far ends (400 and 2500 nm) of the measured wavelength range, as well as in regions dominated by atmospheric water vapor (1350 to 1480 nm and 1780 to 2032 nm).

To convert spectra to canopy trait estimates, trait-specific equations derived by Asner *et al.* (*22*) using partial least squares regression (PLSR) were used. The PLSR uses the continuous spectrum as a single measurement rather than in a band-by-band type of analysis. This approach has been tested and validated in the Peruvian Amazon in previous studies (*22*, *29*, *40*), where foliar chemical traits (e.g., NSC, Chl, Water, and LMA) have been predicted with accuracies ranging from 5 to 18% root mean square error of their mean values (*22*). The resulting maps of LMA, Chl, Water, and NSC of 2-m pixel resolution were previously published for each of the nine sites (*22*).

Single and multitrait functional diversity estimation

Using mapped trait values on a per-pixel basis (4 m^2), we estimated CMT values of remotely sensed traits of LMA, Chl, Water, and NSC by averaging all the values per site. These CMT values showed strong correlations with MAT and elevation and with the community-weighted means of plant traits obtained using field-based methods (see figs. S6 and S7). Using per-pixel values of these four traits, we estimated multitrait functional diversity indices: FRic and FDiv. FRic estimates the volume filled in a multidimensional trait space by a community, whose axes are defined by the four functional traits (*15*). FRic was estimated by calculating the smallest possible convex hull volume that includes all the pixels of a certain neighborhood, whose axes are defined by the functional traits (*14*, *15*). FDiv quantifies how species diverge in their distances from the center of gravity and was calculated using equations by Villeger *et al.* (*15*) adapted by Schneider *et al.* (*21*) when using raster data without species information

$$\Delta\,|\,d\,|\, = \sum_{i=1}^{S} \frac{1}{S} \cdot \left|\, dGi - \overline{dG} \,\right| \tag{1}$$

$$\mathrm{FDiv} = \frac{\overline{dG}}{\Delta\,|\,d\,|\, + \overline{dG}} \tag{2}$$

where S is the number of pixels mapped in the multidimensional space, dGi is the Euclidean distance between the ith pixel and the center of gravity, and $\overline{dG}$ is the average distance of all pixels to the center of gravity (*15*). FDiv varies from 0 to 1, with 1 indicating all pixels lying on a sphere with equal distance to the center of gravity and large trait differences within a community (*15*). Values of FRic and FDiv per site were averaged per site to evaluate linkages between ecosystem productivity and functional diversity. To understand how the four traits were contributing to the overall values of FDiv and FRic, we also calculated these metrics for each single trait (e.g., FRic of LMA, FDiv of NSC). General patterns in CMT values and functional diversity indices with elevation corresponded to trends found using indices derived from field-based measurements (table S2).

Calculating functional diversity area curves

To examine spatial patterns of community assembly, we calculated functional diversity area (FDAR) curves for each site. The observed FDARs within each site were evaluated across increasing neighborhoods of at least 20 m^2 and up to 52,780 m^2 in the largest plot size (e.g., PAN-02, ~5.3 ha; Fig. 2). We selected this method because the study sites showed a variable number of pixels with trait data available (e.g., variable total area per site; fig. S4), likely due to differences in slope and aspect, which may generate a nonrandom distribution of pixels with no data. To account for this within-site variation, for each selected cell (4 m^2), all adjacent cells were added iteratively [contiguous, FDAR type I, as in (*51*)], and we recorded the number of cells sampled (i.e., the total sampled area) at each iteration and the values of FRic and FDiv. This process continued until all cells were sampled in each site and was repeated 1000 times, each time selecting a starting cell at random. The null FDARs within each site were calculated by randomly sampling pixels within sites [type IIIB described in (*51*)], and repeated 1000 times. Thus, 1000 null FDARs were constructed to provide a null expectation for how functional diversity would change with area if trait values were randomly distributed throughout a site. To assess the scale dependency of community assembly processes within each site, we first fitted FDARs using logarithm models [FDAR versus natural log (area) (*51*)] and then compared fitted curves between observed and null models. If observed fitted FDARs of FRic and FDiv are lower than null FDARs (lower than expected by chance), then this would indicate that trait diversity in each site is constrained by environmental filtering (e.g., traits among close neighbor pixels are more similar). In contrast, if observed fitted FDARs are greater than expected by chance, then this suggests that trait diversity may be limited by biotic interactions. Overlapping FDAR curves of null and measured values will indicate that traits in each site are randomly distributed. To assess the effect of spatial scale on community assembly across sites along the elevation gradient, we compared the observed FRic and FDiv values to the randomly assembled communities by calculating the SES according to the method of Gotelli and McCabe (*52*)

$$\mathrm{SES} = \frac{\mathrm{FD}_{\mathrm{observed}} - \mathrm{FD}_{\mathrm{random}}}{\mathrm{FD}_{\mathrm{sd}}} \tag{3}$$

where $\mathrm{FD}_{\mathrm{observed}}$ and $\mathrm{FD}_{\mathrm{random}}$ are mean FD values of the observed and null communities, respectively, in each site, and $\mathrm{FD}_{\mathrm{sd}}$ is the SD of the functional diversity values generated from the 1000 simulations. We calculated mean values, SD, and 95% confidence intervals of SES of FRic and FDiv from 1000 bootstrapped replicate samples. We then used the Wilcoxon signed-rank test to examine whether SES is significantly less, equal, or greater than zero, which indicates the prevalence of trait convergence (environmental filtering), random distribution, or trait divergence (biotic interactions), respectively (*52*). To examine how single-trait functional diversity indices (e.g., FRic of LMA, FDiv of NSC) vary within each site, we also fitted FDAR curves for each of these metrics (see figs. S4 and S5). All analyses were conducted with R 3.4.2 (R Foundation for Statistical Computing, Vienna, AT).

Ecosystem productivity

Sites in the Andes Biodiversity and Ecosystem Research Group network (www.andesconservation.org) have been measured every year for estimations of NPP and GPP following the standard protocol from the GEM Network (http://gem.tropicalforests.ox.ac.uk/projects/aberg). Detailed methods are provided elsewhere (*32*), but briefly within each site, all plant stems ≥10 cm at breast height have been tagged, sized, and identified to species level. Estimation of NPP is based on canopy

litterfall, leaf loss to herbivory, aboveground woody productivity of large trees (≥10 cm), and annual census of wood production of small trees (2 to 10 cm in diameter at breast height), branch turnover of live trees, fine root production, and estimation of coarse root productivity (*22*, *29*, *32*). Estimation of GPP was calculated from the amount of carbon used for NPP and respiration within 1-ha plots. We evaluated the effect of climatic variables, CMT, and functional diversity indices on GPP and NPP rates across elevation. For this, we used the average values per plot of CMT, FRic, and FDiv. We then used a model selection approach to compare all models of predictors using the second-order Akaike's information criterion (AICc) and calculated the ΔAICc values to select the best fitting of the models. ΔAICc was calculated by subtracting the AICc value for the model with the lowest AICc from the AICc value for each model. All models with ΔAICc <2 were considered competitive in explaining the variable response (*53*). To evaluate the relative importance of single-trait functional diversity indices on forest productivity, we correlated each index (e.g., FRic of LMA, FRic of NSC) with NPP and GPP (see table S3).

SUPPLEMENTARY MATERIALS

Supplementary material for this article is available at http://advances.sciencemag.org/cgi/content/full/5/12/eaaw8114/DC1

Fig. S1. Geographic location of the study sites along the Amazon-Andes elevation gradient.
Fig. S2. Variation of remotely sensed CMT values with elevation using a pixel size of 4 m^2.
Fig. S3. Spatial patterns of functional diversity indices in each study site.
Fig. S4. Functional diversity–area relationships across sites for single-trait measurements of FRic.
Fig. S5. Functional diversity–area relationships across sites for single-trait measurements of FDiv.
Fig. S6. Correlations between remotely sensed indices of functional diversity and environmental variables across sites.
Fig. S7. Correlations between CMT values derived from airborne imaging and field-based community-weighted mean traits.
Table S1. Environmental characteristics for the nine sites along the Amazon-to-Andes elevation gradient (215 to 3537 m) in Peru.
Table S2. Relationships between elevation, GPP, and NPP using three sampling approaches of canopy foliar traits.
Table S3. Relationships between GPP and NPP and single-trait functional diversity indices.

REFERENCES AND NOTES

1. S. Diaz, S. Lavorel, F. de Bello, F. Quétier, K. Grigulis, T. M. Robson, Incorporating plant functional diversity effects in ecosystem service assessments. *Proc. Natl. Acad. Sci. U.S.A.* **104**, 20684–20689 (2007).
2. M. W. Cadotte, K. Carscadden, N. Mirotchnick, Beyond species: Functional diversity and the maintenance of ecological processes and services. *J. Appl. Ecol.* **48**, 1079–1087 (2011).
3. E. Garnier, M.-L. Navas, K. Grigulis, *Plant Functional Diversity: Organism Traits, Community Structure, and Ecosystem Properties* (Oxford Univ. Press, 2016).
4. C. Violle, P. B. Reich, S. W. Pacala, B. J. Enquist, J. Kattge, The emergence and promise of functional biogeography. *Proc. Natl. Acad. Sci. U.S.A.* **111**, 13690–13696 (2014).
5. D. Tilman, C. L. Lehman, K. T. Thomson, Plant diversity and ecosystem productivity: Theoretical considerations. *Proc. Natl. Acad. Sci. U.S.A.* **94**, 1857–1861 (1997).
6. D. U. Hooper, F. S. Chapin III, J. J. Ewel, A. Hector, P. Inchausti, S. Lavorel, J. H. Lawton, D. M. Lodge, M. Loreau, S. Naeem, B. Schmid, H. Setala, A. J. Symstad, J. Vandermeer, D. A. Wardle, Effects of biodiversity on ecosystem functioning: A consensus of current knowledge. *Ecol. Monogr.* **75**, 3–35 (2005).
7. Y. Zhang, H. Y. H. Chen, P. B. Reich, Forest productivity increases with evenness, species richness and trait variation: A global meta-analysis. *J. Ecol.* **100**, 742–749 (2012).
8. G. P. Asner, R. E. Martin, D. E. Knapp, R. Tupayachi, C. B. Anderson, F. Sinca, N. R. Vaughn, W. Llactayo, Airborne laser-guided imaging spectroscopy to map forest trait diversity and guide conservation. *Science* **355**, 385–389 (2017).
9. C. P. Carmona, F. de Bello, N. W. H. Mason, J. Lepš, Traits without borders: Integrating functional diversity across scales. *Trends Ecol. Evol.* **31**, 382–394 (2016).
10. J. B. Plotkin, M. D. Potts, D. W. Yu, S. Bunyavejchewin, R. Condit, R. Foster, S. Hubbell, J. LaFrankie, N. Manokaran, L. H. Seng, R. Sukumar, M. A. Nowak, P. S. Ashton, Predicting species diversity in tropical forests. *Proc. Natl. Acad. Sci. U.S.A.* **97**, 10850–10854 (2000).
11. F. He, P. Legendre, Species diversity patterns derived from species–area models. *Ecology* **83**, 1185–1198 (2002).
12. X. Wang, N. G. Swenson, T. Wiegand, A. Wolf, R. Howe, F. Lin, J. Ye, Z. Yuan, S. Shi, X. Bai, D. Xing, Z. Hao, Phylogenetic and functional diversity area relationships in two temperate forests. *Ecography* **36**, 883–893 (2013).
13. A. B. Smith, B. Sandel, N. J. B. Kraft, S. Carey, Characterizing scale-dependent community assembly using the functional-diversity–area relationship. *Ecology* **94**, 2392–2402 (2013).
14. N. W. H. Mason, D. Mouillot, W. G. Lee, J. B. Wilson, Functional richness, functional and functional evenness divergence : The primary of functional components diversity. *Oikos* **1**, 112–118 (2005).
15. S. Villeger, N. W. H. Mason, D. Moullot, New multidimensional functional diversity indices for a multifaceted framework in functional ecology. *Ecology* **89**, 2290–2301 (2008).
16. N. Pérez-Harguindeguy, S. Díaz, E. Garnier, S. Lavorel, H. Poorter, P. Jaureguiberry, M. S. Bret-Harte, W. K. Cornwell, J. M. Craine, D. E. Gurvich, C. Urcelay, E. J. Veneklaas, P. B. Reich, L. Poorter, I. J. Wright, P. Ray, L. Enrico, J. G. Pausas, A. C. de Vos, N. Buchmann, G. Funes, F. Quétier, J. G. Hodgson, K. Thompson, H. D. Morgan, H. terSteege, M. G. A. van der Heijden, L. Sack, B. Blonder, P. Poschlod, M. V. Vaieretti, G. Conti, A. C. Staver, S. Aquino, J. H. C. Cornelissen, New handbook for standardised measurement of plant functional traits worldwide. *Aust. J. Bot.* **61**, 167–234 (2013).
17. S. L. Ustin, D. A. Roberts, J. A. Gamon, G. P. Asner, R. O. Green, Using imaging spectroscopy to study ecosystem processes and properties. *Bioscience* **54**, 523–534 (2004).
18. S. P. Serbin, A. Singh, B. E. McNeil, C. C. Kingdon, P. A. Townsend, Spectroscopic determination of leaf morphological and biochemical traits for northern temperate and boreal tree species. *Ecol. Appl.* **24**, 1651–1669 (2014).
19. G. P. Asner, R. E. Martin, Spectranomics: Emerging science and conservation opportunities at the interface of biodiversity and remote sensing. *Glob. Ecol. Conserv.* **8**, 212–219 (2016).
20. W. Jetz, J. Cavender-Bares, R. Pavlick, D. Schimel, F. W. Davis, G. P. Asner, R. Guralnick, J. Kattge, A. M. Latimer, P. Moorcroft, M. E. Schaepman, M. P. Schildhauer, F. D. Schneider, F. Schrodt, U. Stahl, S. L. Ustin, Monitoring plant functional diversity from space. *Nat. Plants* **2**, 16024 (2016).
21. F. D. Schneider, F. Morsdorf, B. Schmid, O. L. Petchey, A. Hueni, D. S. Schimel, M. E. Schaepman, Mapping functional diversity from remotely sensed morphological and physiological forest traits. *Nat. Commun.* **8**, 1441 (2017).
22. G. P. Asner, R. E. Martin, C. B. Anderson, K. Kryston, N. Vaughn, D. E. Knapp, L. Patrick Bentley, A. Shenkin, N. Salinas, F. Sinca, R. Tupayachi, K. Q. Huaypar, M. M. Pillco, F. D. C. Alvarez, S. Diaz, B. J. Enquist, Y. Malhi, Scale dependence of canopy trait distributions along a tropical forest elevation gradient. *New Phytol.* **214**, 973–988 (2017).
23. G. Vane, A. F. H. Goetz, Terrestrial imaging spectroscopy. *Remote Sens. Environ.* **24**, 1–29 (1988).
24. R. O. Green, M. L. Eastwood, C. M. Sarture, T. G. Chrien, M. Aronsson, B. J. Chippendale, J. A. Faust, B. E. Pavri, C. J. Chovit, M. Soils, M. R. Olah, Imaging spectroscopy and the Airborne visible infrared imaging spectrometer (AVIRIS). *Remote Sens. Environ.* **65**, 227–248 (1988).
25. B. Bayat, C. van der Tol, W. Verhoef, Retrieval of land surface properties from an annual time series of Landsat TOA radiances during a drought episode using coupled radiative transfer models. *Remote Sens. Environ.* 110917 (2018).
26. A. Moreno-Martínez, G. Camps-Valls, J. Kattge, N. Robinson, M. Reichstein, P. van Bodegom, K. Kramer, J. H. C. Cornelissen, P. Reich, M. Bahn, U. Niinemets, J. Peñuelas, J. M. Craine, B. E. L. Cerabolini, V. Minden, D. C. Laughlin, L. Sack, B. Allred, C. Baraloto, C. Byun, N. A. Soudzilovskaia, S. W. Running, A methodology to derive global maps of leaf traits using remote sensing and climate data. *Remote Sens. Environ.* **218**, 69–88 (2018).
27. C. Violle, B. J. Enquist, B. J. McGill, L. I. N. Jiang, C. H. Albert, C. Hulshof, V. Jung, J. Messier, The return of the variance: Intraspecific variability in community ecology. *Trends Ecol. Evol.* **27**, 244–252 (2012).
28. J. Messier, B. J. McGill, M. J. Lechowicz, How do traits vary across ecological scales? A case for trait-based ecology. *Ecol. Lett.* **13**, 838–848 (2010).
29. G. P. Asner, D. E. Knapp, C. B. Anderson, R. E. Martin, N. Vaughn, Large-scale climatic and geophysical controls on the leaf economics spectrum. *Proc. Natl. Acad. Sci. U.S.A.* **113**, E4043–E4051 (2016).
30. G. P. Asner, R. E. Martin, R. Tupayachi, C. B. Anderson, F. Sinca, L. Carranza-Jiménez, P. Martinez, Amazonian functional diversity from forest canopy chemical assembly. *Proc. Natl. Acad. Sci. U.S.A.* **111**, 5604–5609 (2014).
31. C. B. Field, M. J. Behrenfeld, J. T. Randerson, P. Falkowski, Primary production of the biosphere: integrating terrestrial and oceanic components. *Science* **281**, 237–240 (1998).
32. C. A. J. Girardin, Y. Malhi, L. E. O. C. Aragao, M. Mamani, W. Huaraca Huasco, L. Durand, K. J. Feeley, J. Rapp, J. E. Silva-Espejo, M. Silman, N. Salinas, Net primary productivity allocation and cycling of carbon along a tropical forest elevational transect in the Peruvian Andes. *Glob. Chang. Biol.* **16**, 3176–3192 (2010).
33. B. J. Enquist, L. Patrick-Bentley, A. Shenkin, B. Maitner, V. Savage, S. Michaletz, B. Blonder, V. Buzzard, T. E. B. Espinoza, W. Farfan-Rios, C. E. Doughty, G. R. Goldsmith, R. E. Martin,

N. Salinas, M. Silman, S. Diaz, G. P. Asner, Y. Malhi, Assessing trait-based scaling theory in tropical forests spanning a broad temperature gradient. *Glob. Ecol. Biogeogr.* **26**, 1357–1373 (2017).
34. N. M. Fyllas, L. Patrick-Bentley, A. Shenkin, G. P. Asner, O. K. Atkin, S. Diaz, B. J. Enquist, W. Farfan-Rios, E. Gloor, R. Guerrieri, W. H. Huasco, Y. Ishida, R. E. Martin, P. Meir, O. Phillips, N. Salinas, M. Silman, L. K. Weeransinghe, J. Zaragoza-Castells, Y. Malhi, Solar radiation and functional traits explain the decline of forest primary productivity along a tropical elevation gradient. *Ecol. Lett.* **20**, 730–740 (2017).
35. I. J. Wright, P. B. Reich, M. Westoby, D. D. Ackerly, Z. Baruch, F. Bongers, J. Cavender-Bares, T. Chapin, J. H. C. Cornelissen, M. Diemer, J. Flexas, E. Garnier, P. K. Groom, J. Gulias, K. Hikosaka, B. B. Lamont, T. Lee, W. Lee, C. Lusk, J. J. Midgley, M. L. Navas, U. Niinemets, J. Oleksyn, N. Osada, H. Poorter, P. Poot, L. Prior, V. I. Pyankov, C. Roumet, S. C. Thomas, M. G. Tjoelker, E. J. Veneklaas, R. Villar, The worldwide leaf economics spectrum. *Nature* **428**, 821–827 (2004).
36. G. P. Asner, R. E. Martin, Canopy phylogenetic, chemical and spectral assembly in a lowland Amazonian forest. *New Phytol.* **189**, 999–1012 (2011).
37. G. Hoch, A. Richter, C. Körner, Non-structural carbon compounds in temperate forest trees. *Plant Cell Environ.* **26**, 1067–1081 (2003).
38. E. Weiher, P. A. Keddy, Assembly rules, null models, and trait dispersion: New questions from old patterns. *Oikos* **74**, 159–164 (1995).
39. J. P. Grime, Trait convergence and trait divergence in herbaceous plant communities: Mechanisms and consequences. *J. Veg. Sci.* **17**, 255–260 (2006).
40. G. P. Asner, R. E. Martin, C. B. Anderson, D. E. Knapp, Quantifying forest canopy traits: imaging spectroscopy versus field survey. *Remote Sens. Environ.* **158**, 15–27 (2015).
41. J. Kattge, S. Díaz, S. Lavorel, I. C. Prentice, P. Leadley, G. Bönisch, E. Garnier, M. Westoby, P. B. Reich, I. J. Wright, J. H. C. Cornelissen, C. Violle, S. P. Harrison, P. M. Van Bodegom, M. Reichstein, B. J. Enquist, N. A. Soudzilovskaia, D. D. Ackerly, M. Anand, O. Atkin, M. Bahn, R. Baker, D. Baldocchi, R. Bekker, C. C. Blanco, B. Blonder, W. J. Bond, R. Bradstock, D. E. Bunker, F. Casanoves, J. Cavender-Bares, J. Q. Chambers, F. S. Chapin III, J. Chave, D. Coomes, W. K. Cornwell, J. M. Craine, B. H. Dobrin, L. Duarte, W. Durka, J. Elser, G. Esser, M. Estiarte, W. F. Fagan, J. Fang, F. Fernández-Méndez, A. Fidelis, B. Finegan, O. Flores, H. Ford, D. Frank, G. T. Freschet, N. M. Fyllas, R. V. Gallagher, W. A. Green, A. G. Gutierrez, T. Hickler, S. I. Higgins, J. G. Hodgson, A. Jalili, S. Jansen, C. A. Joly, A. J. Kerkhoff, D. Kirkup, K. Kitajima, M. Kleyer, S. Klotz, J. M. H. Knops, K. Kramer, I. Kühn, H. Kurokawa, D. Laughlin, T. D. Lee, M. Leishman, F. Lens, T. Lenz, S. L. Lewis, J. Lloyd, J. Llusià, F. Louault, S. Ma, M. D. Mahecha, P. Manning, T. Massad, B. E. Medlyn, J. Messier, A. T. Moles, S. C. Müller, K. Nadrowski, S. Naeem, Ü. Niinemets, S. Nöllert, A. Nüske, R. Ogaya, J. Oleksyn, V. G. Onipchenko, Y. Onoda, J. Ordoñez, G. Overbeck, W. A. Ozinga, S. Patiño, S. Paula, J. G. Pausas, J. Peñuelas, O. L. Phillips, V. Pillar, H. Poorter, L. Poorter, P. Poschlod, A. Prinzing, R. Proulx, A. Rammig, S. Reinsch, B. Reu, L. Sack, B. Salgado-Negret, J. Sardans, S. Shiodera, B. Shipley, A. Siefert, E. Sosinski, J.-F. Soussana, E. Swaine, N. Swenson, K. Thompson, P. Thornton, M. Waldram, E. Weiher, M. White, S. White, S. J. Wright, B. Yguel, S. Zaehle, A. E. Zanne, C. Wirth, TRY—A global database of plant traits. *Glob. Chang. Biol.* **17**, 2905–2935 (2011).
42. H. Bruelheide, J. Dengler, B. Jiménez-Alfaro, O. Purschke, S. M. Hennekens, M. Chytrý, V. D. Pillar, F. Jansen, J. Kattge, B. Sanderl, I. Aubin, sPlot–A new tool for global vegetation analyses. *J. Veg. Sci.* **30**, 161–186 (2018).
43. B. S. Maitner, B. Boyle, N. Casler, R. Condit, J. Donoghue, S. M. Durán, D. Guaderrama, C. E. Hinchliff, P. M. Jørgensen, N. J. Kraft, B. McGill, The Bien R package: A tool to access the botanical information and ecology network (BIEN) database. *Methods Ecol. Evol.* **9**, 373–379 (2018).
44. L. Guanter, H. Kaufmann, K. Segl, S. Foerster, C. Rogasss, S. Chabillat, T. Kuester, A. Hollstein, G. Rossner, C. Chlebek, C. Straif, S. Fischer, S. Schrader, T. Storch, U. Heiden, A. Mueller, M. Bachmann, H. Mühle, R. Müller, M. Habermeyer, A. Ohndorf, J. Hill, H. Budenbaum, P. Hostert, S. van der Linden, P. J. Leitão, A. Rabe, R. Doerffer, H. Krasemann, H. Xi, W. Mauser, T. Hank, M. Locherer, M. Rast, K. Staenz, B. Sang, The EnMAP spaceborne imaging spectroscopy mission for earth observation. *Remote Sens. (Basel)* **7**, 8830–8857 (2015).
45. Z. Tang, W. Xu, G. Zhou, Y. Bai, J. Li, X. Tang, D. Chen, Q. Liu, W. Ma, G. Xiong, H. He, Patterns of plant carbon, nitrogen, and phosphorus concentration in relation to productivity in China's terrestrial ecosystems. *Proc. Natl. Acad. Sci. U.S.A.* **115**, 4033–4038 (2018).
46. M. Neyret, L. P. Bentley, I. Oliveras, B. S. Marimon, B. H. Marimon-Junior, E. A. de Oliveira, F. B. Passos, R. C. Ccoscco, J. dos Santos, S. M. Reis, P. S. Morandi, G. R. Paucar, A. R. Caceres, Y. V. Tejeira, Y. Y. Choque, N. Salinas, A. Shenkin, G. P. Asner, S. Diaz, B. J. Enquist, Y. Malhi, Examining variation in the leaf mass per area of dominant species across two contrasting tropical gradients in light of community assembly. *Ecol. Evol.* **6**, 5674–5689 (2016).
47. I. Šímová, B. Sandel, B. J. Enquist, S. T. Michaletz, J. Kattge, C. Violle, B. J. McGill, B. Blonder, K. Engemann, R. K. Peet, S. K. Wiser, The relationship of woody plant size and leaf nutrient content to large-scale productivity for forests across the Americas. *J. Ecol.* **107**, 2278–2290 (2019).
48. M. Zhao, F. A. Heinsch, R. R. Nemani, S. W. Running, Improvements of the MODIS terrestrial gross and net primary production global data set. *Remote Sens. Environ.* **95**, 164–176 (2004).
49. B. Sakschewski, W. von Bloh, A. Boit, L. Poorter, M. Peña-Claros, J. Heinke, J. Joshi, K. Thonicke, Resilience of Amazon forests emerges from plant trait diversity. *Nat. Clim. Change* **6**, 1032–1036 (2016).
50. G. P. Asner, D. E. Knapp, J. Boardman, R. O. Green, T. Kennedy-Bowdoin, M. Eastwood, R. E. Martin, C. Anderson, C. B. Field, Carnegie Airborne Observatory-2: Increasing science data dimensionality via high-fidelity multi-sensor fusion. *Remote Sens. Environ.* **124**, 454–465 (2012).
51. S. M. Scheiner, Six types of species-area curves. *Glob. Ecol. Biogeogr.* **12**, 441–447 (2003).
52. N. J. Gotelli, D. J. McCabe, Species co-occurrence: A meta-analysis of j. m. diamond's assembly rules model. *Ecology* **83**, 2091–2096 (2002).
53. D. R. Anderson, *Model Based Inference in the Life Sciences: A Primer on Evidence* (Springer Science & Business Media, 2008).

Acknowledgments: We thank two anonymous referees for constructive comments on earlier drafts. This work is a product of the Global Ecosystems Monitoring (GEM) network (gem.tropicalforests.ox.ac.uk), the Andes Biodiversity and Ecosystem Research Group (andesresearch.org), the Amazon Forest Inventory Network RAINFOR (www.rainfor.org), and the Carnegie Spectranomics Project (spectranomics.carnegiescience.edu) research consortia. **Funding:** Field campaigns were funded by grants to Y.M. from the UK Natural Environment Research Council (grants NE/J023418/1, NE/J023531/1, and NE/F002149/1), the European Research Council Advanced Investigator (grant GEM-TRAITS 321131), and the Gordon and Betty Moore Foundation to Y.M., M.R.S., and G.P.A. Carnegie Airborne Observatory (CAO) flights, data processing, and analyses were supported by a grant to G.P.A. from the John D. and Catherine T. MacArthur Foundation. The CAO is made possible by grants and donations to G.P.A. from the Avatar Alliance Foundation, Margaret A. Cargill Foundation, David and Lucile Packard Foundation, Gordon and Betty Moore Foundation, Grantham Foundation for the Protection of the Environment, W. M. Keck Foundation, John D. and Catherine T. MacArthur Foundation, Andrew Mellon Foundation, Mary Anne Nyburg Baker and G. Leonard Baker Jr., and William R. Hearst III. This work was supported by NSF grant DEB1457812 (to B.J.E., L.P.B., G.P.A., and V.M.S.) and NSF grant DEB (LTREB) 1754647 (to M.R.S.). **Author contributions:** S.M.D. and B.J.E designed the research. Y.M. conceived and funded the original trait data collection, and L.P.B., A.S., G.P.A., R.E.M., S.D., N.S., M.R.S. gathered the stand and functional traits data. G.P.A. and R.E.M. carried out the remote sensing data collection, processing, and analyses. S.M.D. analyzed the data. B.S.M. contributed to analytical tools used in the analysis. S.M.D. wrote the first draft of the manuscript, and all authors contributed substantially to the revisions. **Competing interests:** The authors declare that they have no competing interests. **Data and materials availability:** All data used to generate the main analyses and figures are available on GitHub (https://github.com/smduranm/SCI_ADV_aw8114). Spatial information of each plot and original chemical maps of the plant traits can be requested to J. Heckler at the Global Airborne Observatory Program at Arizona State University (jheckler@asu.edu) and will be pending of a completed material transfer agreement. Additional data related to this paper may be requested from the authors.

Submitted 26 January 2019
Accepted 26 September 2019
Published 4 December 2019
10.1126/sciadv.aaw8114

Citation: S. M. Durán, R. E. Martin, S. Díaz, B. S. Maitner, Y. Malhi, N. Salinas, A. Shenkin, M. R. Silman, D. J. Wieczynski, G. P. Asner, L. P. Bentley, V. M. Savage, B. J. Enquist, Informing trait-based ecology by assessing remotely sensed functional diversity across a broad tropical temperature gradient. *Sci. Adv.* **5**, eaaw8114 (2019).

Science Advances

Informing trait-based ecology by assessing remotely sensed functional diversity across a broad tropical temperature gradient

Sandra M. Durán, Roberta E. Martin, Sandra Díaz, Brian S. Maitner, Yadvinder Malhi, Norma Salinas, Alexander Shenkin, Miles R. Silman, Daniel J. Wieczynski, Gregory P. Asner, Lisa Patrick Bentley, Van M. Savage and Brian J. Enquist

Sci Adv **5** (12), eaaw8114.
DOI: 10.1126/sciadv.aaw8114